Energy & Environmental Science

Electrical decoupling of microbial electrochemical reactions enables spontaneous H2 evolution

Journal:	*Energy & Environmental Science*
Manuscript ID	EE-COM-08-2019-002571.R1
Article Type:	Communication
Date Submitted by the Author:	29-Sep-2019
Complete List of Authors:	Chen, Xi; Princeton University, Department of Civil and Environmental Engineering Lobo, Fernanda; Universidade Federal do Ceara Bian, Yanhong; Princeton University, Department of Civil and Environmental Engineering Lu, Lu; Princeton University, Department of Civil and Environmental Engineering Chen, Xiaowen; National Renewable Energy Lab, national bioenergy center Tucker, Melvin; National Renewable Energy Laboratory, National Bioenergy Center Wang, Yuxi; Columbia University, The Earth Institute and School of International and Public Affairs Ren, Zhiyong; Princeton University, Department of Civil and Environmental Engineering

Electrical decoupling of microbial electrochemical reactions enables spontaneous H_2 evolution

Xi Chen[1], Fernanda Leite Lobo[2], Yanhong Bian,[1] Lu Lu[1], Xiaowen Chen[3], Melvin P. Tucker[3], Yuxi Wang[4], Zhiyong Jason Ren [1*]

[1] Department of Civil and Environmental Engineering and Andlinger Center for Energy and the Environment, Princeton University, Princeton, NJ 08544, United States

[2] Departamento de Engenharia Hidráulica e Ambiental, Universidade Federal do Ceará, Brazil

[3] National Bioenergy Center, National Renewable Energy Laboratory, 15013 Denver West Parkway, Golden, United States

[4] The Earth Institute and School of International and Public Affairs, Columbia University, New York, NY 10027, United States

*Correspondence: zjren@princeton.edu

Broader context box

H_2 complements renewable electricity as a renewable fuel carrier and chemical building block, but H_2 evolution is an endothermic reaction that requires external energy input to close the thermodynamic gap of water splitting. This study demonstrated unassisted H_2 evolution by using an electrical decoupling strategy with a tailored power management system (PMS), which can overcome the thermodynamic gap and achieve uphill reactions by electrically decoupling the reactions and temporarily storing the energy generated from anodic organic oxidization reactions. This approach greatly simplifies electrochemical H_2 production systems and advances a new H_2 economy.

ABSTRACT

Hydrogen evolution is not a spontaneous reaction, so current electrochemical H_2 systems either require an external power supply or use complex photocathodes. We present in this study that by using electrical decoupling H_2 can be produced spontaneously from the wastewater. A power management system (PMS) circuit was deployed to decouple bioanode organic oxidation from abiotic cathode proton reduction in the same electrolyte. The special PMS consisted a boost converter and an electromagnetic transformer, which harvested energy from the anode followed by voltage magnification from 0.35 V to 2.2~2.5 V, enabling *in situ* H_2 evolution for over 96 h without consuming any external energy. This proof-of-concept demonstrated a cathode faradic efficiency of 91.3% and a

maximum overall bioelectrochemical H_2 conversion efficiency of 28.9%. This approach allows true self-sustaining wastewater to H_2 evolution, and system performance can be improved via PMS and reactor optimization.

KEYWORDS

Hydrogen, decoupling, microbial electrolysis, power management system, boost converter, flyback converter

INTRODUCTION

Hydrogen is a desired fuel and medium for fuel cell vehicles and largescale energy storage solutions, and it is an essential chemical building block for industries that produce fertilizers, polymers, plastics, pharmaceuticals, and many critical products.[1-4] Plus, hydrogen provides a complementary alternative to renewable electricity, and it can be produced using renewables such as solar and wind via water splitting or biomass and wastewater via fermentation and microbial electrolysis.[5-8]

Traditional water splitting requires a theoretical 1.23 V to overcome the thermodynamic barrier ($H_2O \rightarrow H_2 + 0.5\ O_2$, ΔG^0 = 237.13 kJ/mol), and in reality 1.8~2.0 V is used to overcome the potential losses associated with internal resistance, junction potential, and overpotential on electrode surface.[9, 10] Electrochemical H_2 production therefore has always relied on an external bias that requires energy input and additional infrastructure. This is true even for sustainable H_2 production from renewable sources, such as artificial photosynthesis (APS) that utilizes solar energy to substitute part of the electricity input,[11, 12] as well as microbial electrolysis cells (MEC) that employ a variety of organic matters as the electron donor to reduce external voltage demand.[7, 13, 14] Direct photoelectrolysis of water at the interface of semiconductor and electrolyte has been a popular APS pathway, but an external bias is still needed because

most semiconductors, such as Si, InP, and GaAs, do not produce sufficient voltage to drive water-splitting due to the larger junction gap of 1.6 to 2.3 eV.[15-18] This external bias can be greatly reduced when the anodic water oxidation is replaced by microbial organic oxidization, because bacteria utilizes the chemical energy embedded in organics to compensate the energy required for anode oxidation, and as a result the thermodynamic driving force required for H_2 production dramatically reduced from 1.23 V (water oxidation) to 0.12 V (acetate oxidation).[18, 19] Additionally, as a variety of organics, even wastewater, can be oxidized by microbial metabolism, people attempted to approach a goal of sustainable fuel supply based on the enormous and readily achievable waste streams produced in human society.[20] However, the aforementioned H_2 production from wastewater still relied on additional power such as electricity or solar, which is not a true waste-to-hydrogen situation. In a previous work by Suraniti, et al, an enzymic biofuel cell was coupled with water electrolysis to achieve H_2 production in a glucose medium.[21] An electrical booster and an electromagnetic transformer were included in the external circuit to condition the voltage produced by the biofuel cell and drive water electrolysis. The study demonstrated that electric circuits could help overcome the thermodynamic gap and achieve uphill reactions, though the system was only operated for 200 min.[21] There has been no study that achieved spontaneous H_2 evolution from wastewater without any external energy input.

Considering the limited and intermittent nature of power supply from renewable sources, a new strategy that decouples the two half electrochemical reactions in an electrolyzer was recently proposed by inserting a reversible redox mediator into the electrolyzer. Hydrogen evolution reaction (HER) on the cathode and oxygen evolution reaction (OER) on the anode were not directly coupled rather mediated by the reversible reactions of a mediator, so the HER and OER could be decoupled and occur at different specific production rates.[4, 22, 23] Several mediators such as polyoxometalate phosphomolybdic acid, V^{3+}, and nickel (oxy)hydroxides, have been demonstrated capable of decoupling the electrochemical reactions of water splitting.[22, 24, 25] The concept of decoupling was originally proposed to separate the OER and HER in order to prevent the crossover of produced O_2 and H_2,[4] but we hypothesize here the different reaction rates on the anode and cathode enabled by the decoupling strategy may open up opportunities for *in situ* energy storage and utilization. The reactions being decoupled don't have to be the OER and HER but could be any redox pair in an electrochemical cell.

In this study, we demonstrate the proof-of-concept that spontaneous H_2 evolution could be achieved from wastewater by using a tailored power management system (PMS) to decouple the electrochemical reactions with O_2 as a redox

mediator. Since the electrochemical reactions occurred in one common electrolyte, water splitting won't be able to occur spontaneously due to the aforementioned thermodynamic barrier, but this barrier can be overcome by electrically decoupling the reactions and temporarily storing the energy generated from anodic organic oxidization reactions in the PMS. During this time, the PMS raised the voltage output high enough to enable spontaneous H_2 evolution on the cathode. Because no external energy (even sunlight) was applied to the system, rather the H_2 revolution was solely driven by the PMS, which accumulated energy from the anodic bio-oxidation of the wastewater, making the overall process spontaneous and exothermic. In addition, we characterized the mechanisms of the decoupling strategy, PMS design, reactor performance, and the energy flow.

RESULTS AND DISCUSSION

Principle of the electrical decoupling that enabled spontaneous H_2 evolution

Decoupling strategies are used to do more with less, and a free pulley example is used here to explain the decoupled electrochemical reactions that enabled the endothermic H_2 evaluation without an external power supply. **Fig. 1A** shows that when a balloon is directly connected to a basket, a higher lifting force is required to lift the load. This is similar as a conventional electrochemical cell, which requires high enough external voltage to overcome the thermodynamic barrier of H_2 evolution. **Fig. 1A** shows a traditional microbial electrolysis cell (MEC), where

the theoretical cell electromotive force (E_{emf} (V)) is -0.12 V (-0.41-(-0.29 V)), indicating that a > 0.12 V external bias is needed to overcome the thermodynamic barrier for H_2 production. In reality, the external voltage used was 0.6-1.2 V due to overpotential and other losses.[7, 8, 13]

In contrast, **Fig. 1B** shows when a free pulley is used, a much smaller effort is needed to lift the same load. This is analogous to the principle used in this study, where the O_2 mediator and a power management system (PMS) served as an "electric pulley" to decouple the anodic and cathodic reactions and transform the driving force. By inserting a pair of O_2 reduction (blue) and oxidation (pink) electrodes into the reactor, the bioanode organic oxidation was decoupled from the cathode proton reduction, and the PMS then enables a temporary storage of the electrical energy harvested in the organic oxidization-O_2 reduction reaction, which was termed as "energy generation part", and raised the output potential to realize the spontaneous "H_2 evolution part", which was the newly formed H_2O oxidization-proton reduction reaction. The PMS had dual functions: magnifying the output voltage of the energy generation part, and transfer the harvested energy electromagnetically thus achieve DC isolation between the two pairs of electrodes. This is significant because without the electrical decoupling using the PMS, the two electrochemical reactions in one common electrolyte cannot perform separately due to their intrinsic electric connection via the solution.

The PMS primarily consisted of an energy harvesting circuit and an electromagnetic transformer placed on a specially designed flyback converter.[21, 26] The energy harvesting circuit can harvest the energy generated from the bioanode, generally at the maximum power point,[27] so there is enough potential to power the whole PMS without the need for any external energy. The flyback converter is a key component that allows DC isolation that electrically decouples the chemical reactions. In the control experiment using just the energy harvesting circuit to connect the external circuit of two reactions, a stable output voltage was achieved from the energy generation part but no current was detected in the H_2 evolution part. Without DC isolation, all the chemical oxidation and reduction reactions are connected in the electrolyte as well as through the circuit to a same electrical reference, making the whole system short circuited. The primary and secondary windings of the electromagnetic transformer are not electrically connected, so the circuits of the energy generation part and the H_2 evolution part are DC isolated which enables two different electrical references: anode oxidation (GND1) and cathode reduction (GND2) as shown in **Figure 2A**, hence avoiding the short circuit between the PMS input and output. The input energy from the energy generation part is periodically transferred from the first winding to the second winding of the transformer, and therefore the flyback converter is operated in a charge-discharge cycle to power H_2 generation.[27, 28]

175

176 **The input and output of the decoupled circuit**

177 The flyback converter's capability in DC isolation and energy transfer were
178 presented via voltage input and output measured by an oscilloscope (**Figure 2B,**
179 **2C**). **Figure 2B** presents the output voltage from the energy harvesting circuit with
180 pulse-frequency modulation (PFM) control by using constant duty cycle and
181 variable frequency that is a modulation technique used in low power energy
182 harvesters. The same voltage profile was also the flyback converter's voltage
183 input, which was boosted to 2.16 V with a considerable ripple caused by the
184 production of gas bubbles on the cathode surface. The boosted voltage varied
185 according with the setting of the energy harvesting circuit control and the
186 performance of energy generation part. This boosted voltage was able to power
187 the flyback and at the same time be isolated to further support H_2 evolution.
188 **Figure 2C** shows a fairly constant voltage that represents the flyback converter's
189 output voltage. This voltage (2.32 V) is similar as the flyback input voltage (2.16
190 V), because the flyback converter's function in this study is DC isolation and
191 electromagnetic energy transfer. The output voltage was kept stable at around 2.3
192 V with a different electrical reference from the energy generation part (**Fig. 2C**).
193 The voltage sign is deliberately measured negative to power the water splitting for
194 H_2 production.

195

The PFM control used in the circuit design in this study could keep the output voltage of the energy generation part at a stable 0.35 V level, which ensures a stable input for the H_2 evolution part and leads to a 2.3 V output throughout the operation cycle. As a result, H_2 could be continuously generated till the complete consumption of organic substrates. This demonstrates the stability and practicability of this system. Without such PFM control, the energy generation part would output a decreasing voltage over time. The input voltage of H_2 evolution part, which was boosted at a fixed magnification, would decrease correspondingly and soon result in the interrupt of H_2 production when the transferred voltage could no longer support water splitting. Considering unlimited wastewater supply in actual situation, this system would be able to achieve long-term spontaneous H_2 production. When wastewater was replaced every 4 days to ensure stable supply of substrates, multiple cycles of operation without external energy supply were achieved without apparent performance decay (**SI, Figure S1**).

Performance of the system

Each test of the system was operated in the synthetic wastewater (an acetate medium) for 96 hours, and stable electric output and H_2 generation were observed (**Figure 3**). **Figure 3A** shows H_2 bubbles were continuously produced from the cathode at a high rate without any external energy input (see the video clip in **SI**). Stable H_2 generation was observed during the experiment, credited to

stable current input for H_2 evolution (**Figure 3B**). The time-course output voltage of energy generation part was kept consistent at the maximum power point of 0.35 V by the PFM control circuit, while a 2.2~2.5 V voltage output was obtained from the PMS and applied on the H_2 evolution part (**Figure 3C**). This *in situ* conversion of voltage enabled spontaneous H_2 evolution without an external assistance. Because of voltage magnification, the current reduced from 2.0~2.8 mA in the energy generation part to less than 0.1 mA in the H_2 evolution part, conforming to the principle of total energy conservation (**Figure 3D**). Considering the degradation of organic substance in the anode, the conductivity of medium decreased from 12.84 to 9.86 mS/cm, which led to the increase of internal resistance between the anode and cathode of the energy harvesting part, thus the current output gradually decreased along the cycle. Accordingly, the current profiles on input to the hydrogen evolution part and output from the energy generation part were analogous in shape (**Figure 3D**). To avoid the interfere of the ripples in data, average powers during each 24 h were used to show the power output/input of the energy generation/H_2 evolution parts, respectively (**Figure 3E**). The power generation from organic degradation in the anode ranged from 0.67 to 0.95 mW during the operation, which averaged at 0.76, 0.72, 0.74, and 0.68 mW within each day, respectively. From such energy input, average outputs of 0.15, 0.14, 0.14, and 0.12 mW were used for water splitting via the PMS magnification and transformation during the same operation period (**Figure**

3E). Over 90% of the acetate in the anode was removed, representing a satisfactory treatment of wastewater. The corresponding Coulombic efficiency was 34.2%. The spontaneous H_2 production rate was 2.75 mL/L/day, and the yield was 0.034 mol H_2/mol acetate. This is lower than reported abiotic or microbial electrolysis process (which could range from 10^1 to 10^5 mL/L/day) due to the absence of external voltage application,[5-8] but comparable to previous reports that used enzymes to generate H_2 from glucose (0.051 mol H_2/mol glucose).[21] Based on the total coulomb input into the H_2 evolution circuit, a H_2 production rate of 3.05 mL/L/day could be obtained per operation cycle with a corresponding Faradic Efficiency of 91.3%. To further improve H_2 production performance, the O_2 evolution anode maby be replaced by a bioanode to reduce the thermodynamic gap of the H_2 evolution part. In this way, a lower input voltage and a larger current would be realized to produce H_2 at higher rates and efficiencies. The main advantages of this study however come from the low operational cost, zero energy input, and long sustainability with concurrent benefits of wastewater treatment.

System efficiency and energy analysis

Figure 4 shows the energy efficiency and energy flow of the system. During a typical 96-h operation, an average 0.73 mW of power was generated from the energy generation part during organic degradation on the bioanode. This power

was subsequently consumed by the energy harvesting circuit, the flyback converter, and the H_2 evolution reaction, respectively. **Figure 4A** demonstrates the energy harvesting circuit had an efficiency of 70% (a fixed value by the manufacturer), and the flyback converter had an efficiency of 45.1%, resulted a maximum efficiency of 31.6% by the PMS. However, due to the ripple in current, the efficiency of the PMS fluctuated and averaged at 19.2% with a corresponding average flyback efficiency of 27.4% (**Figure 4A**). The energy flow presented in **Figure 4B, 4C** shows how much power each part of the system consumed to enable the spontaneous H_2 generation from organic matter. In the case when PMS showed a maximum efficiency, a highest power of 0.25 mW was achieved in the H_2 evolution reaction, representing 31.6 % of the produced power from the energy generation part (**Figure 4B**). The energy harvesting circuit consumed 0.24 mW to drive the magnification of voltage. This circuit is a commercial circuit by Texas Instruments with a known power consumption.[27] The flyback converter required another 0.30 mW to operate, which occupied the most fraction, 38.0%, of the total produced power. The losses in the flyback converter were primarily on the transformer and diode, where the transformer incurred core and conduction losses as well as resistance on windings, while the diode presented losses on threshold voltage and forward resistance. However, to compare with similar flyback converter designed for other low power energy systems, the > 25% energy conversion efficiency was normal.[26] **Figure 4C** showed the energy flow

calculated using average PMS efficiency. In average, 0.14 mW was used by the H_2 evolution reaction, representing 19.2% of the total generated power. Further considering the 91.3% H_2 generation efficiency on the cathode, the overall conversion efficiency could reach a maximum of 28.9% and an average of 17.5%.

Even though the efficiency could be improved, this proof-of-concept study demonstrates that without this electric decoupling the electrochemical reactions and temporary energy storage/transfer would not be achieved, not to mention spontaneous H_2 evolution. This invention itself saved energy and presumably cost compared with previous studies that used external power source to realize water splitting. The system efficiency can be further improved by improving the efficiencies of both the energy harvesting circuit and the flyback converter, using bioanode to replace the OER anode to reduce the load of the PMS, and optimizing the configuration design to reduce the internal resistance.

CONCLUSIONS

This study demonstrates an electric decoupling method that enabled spontaneous H_2 production from organic waste treatment. The PMS decoupled bioanode organic oxidation from cathode proton reduction in the same electrolyte. The tailored PMS realized this decoupling by using an energy harvesting circuit to collect the energy generated from organic chemicals and magnified the voltage

from 0.35 V to 2.2~2.5 V *in situ*, where the electromagnetic transformer transferred the energy and allowed water splitting without consuming any external energy. Without such decoupling strategy, some types of external energy input such as an external power supply, another renewable energy system, or sunlight incidence, is necessary to close the thermodynamic gap of water electrolysis. Thus, a real self-sustaining wastewater-to-hydrogen spontaneous conversion was achieved. The system demonstrated good conversion efficiency, with the H_2 producing rate of 2.75 mL/L/day, the cathode faradic efficiency of 91.3%, and the maximum overall bioelectrochemical energy to H_2 conversion efficiency of 28.9%.

EXPERIMENTAL PROCEDURE

Power management system (PMS)

The tailored PMS was designed to have two major circuits (**Figure 2**). One circuit was for energy harvesting that collected the electricity generated from organic degradation and boosted the input voltage by >6 times as the output voltage. This integrated energy harvesting circuit utilized a pulse-frequency modulation boost converter/charger (BQ25505, Texas Instruments Inc.) to boost the voltage from 0.35 V (the output voltage of energy generation part) to ~2.2 V to power water electrolysis. The minimum voltage necessary to power the BQ25505 is 0.1 V per the manufacturer's instruction, and no external energy was needed for the operation of this circuit. The second circuit was a flyback converter (a

transformer-based DC-DC converter), which was designed specifically for this study using the theory of Pulse-Width Modulated DC-DC Power Converters by Marian K Kazimiercizuk.[29] The flyback converter built for this study (Figure 2, the blue doted box) comprises of a transformer 78601/9MC from Murata Power Solutions (*T*), a Fast Switching Diode Vishay 1N4448 (*D*), a capacitor 100uF (*C*), a MOSFET 3NL01C (*S*). The control was performed by an oscillator/timer TS3003 from Silicon Lab, delivering a Pulse-Width Modulation in 9 kHz of frequency and a duty cycle of 50%. Such oscillator was powered by the 2.3 V output of the energy harvesting circuit, so no external energy was needed.

The transformer magnetizing inductance L_m played a critical role on PMS energy storage because even if no current was flowing at the secondary windings of the transformer, current would flow through the primary on L_m (Figure 2A), and that is how the PMS in this study was storing the magnetic energy. When the MOSFET (*S*) was ON and the diode (*D*) was OFF, the primary of the transformer was storing energy on L_m. While when the MOSFET (*S*) was OFF and the diode (*D*) was ON, energy was transferred from the primary to the secondary windings of the transformer and then passed to the capacitor (*C*). This cycle of energy storage and transfer in high frequency (9kHz on the flyback converter and variable frequency for the energy harvesting circuit using a PFM) enabled the spontaneous water splitting without any external energy.

343

344 **System construction**

345 The microbial electrochemical water electrolyzer contained three functional
346 components, the energy generation part, the PMS (introduced in the previous
347 section), and the H_2 evolution part (**Figure 1**). All these components were
348 assembled in a cubic-shape reactor that had a 7 cm inner diameter and 5 cm
349 depth (Perspex) (**SI, Figure S2**). The energy generation part consisted of a
350 bioanode that employ bacteria to degrade organics to generate electrons, and an
351 abiotic Pt/C air cathode that conducted O_2 reduction. The anode was made of a
352 carbon brush (5 cm diameter and 5 cm length) to support biofilm growth and
353 conduct electrons. The air cathode of 7 cm in diameter was made from one
354 carbon base layer, four polytetrafluoroethylene diffusion layers and one catalyst
355 layer (0.5 mg Pt/cm^2).[30] The catalyst layer faced electrolyte and the diffusion layer
356 was in contact with air. A Ag/AgCl reference electrode (RE-5B, BASi, IN, USA;
357 +0.210 V versus standard hydrogen electrode, 25 ℃) was used for electrical
358 character measurement. The H_2 evolution part included a platinum wire anode for
359 O_2 generation and a platinum microelectrode (MF-2005, BASi, IN, USA) for H_2
360 evolution. The O_2 generation electrode was placed adjacent to the
361 aforementioned air cathode to allow O_2 consumption. A piece of glass fiber was
362 placed in between the O_2 generation anode and the H_2 evolution cathode to
363 further secure the separation of the produced H_2 from any remaining O_2. The

whole electrolyzer was sealed up tightly using screws, rubber gasket and glue. An air bag was connected on the top of the reactor for gas collection.

System operation

Figure 1B shows the system schematic and electrode connection. The external circuit of the bioanode connected to the O_2 reduction cathode via the energy harvesting circuit in the PMS, while the external circuit of the water oxidation anode connected to the H_2 evolution cathode via the flyback converter in the PMS. The bioanode was inoculated using anaerobic sludge obtained from a municipal wastewater treatment plant.[31] The bioanode was grown in a microbial electrolysis cell using a nickel-foam cathode under an applied voltage of 0.8 V for 30 days before transferring to the experiment reactor.[32] During the time of acclimation, the bioanode was enriched with electroactive biofilm and could stably support a current around 10 mA. The bioanode could support a stable voltage output of 0.35 V and maintained a stable current output during multiple cycles of operation (**SI, Figure S1**).The electrolyte utilized for conducting experiments in this study contained (per liter): 1.64 g NaAc, 0.31 g NH_4Cl, 0.1 g $CaCl_2$, 0.1 g $MgCl_2$, and 100 mM phosphate buffer.[33] The reactor was operated in fed-batch mode with a cycle time of 96 h. The operation of the PMS was solely powered by the electricity generated from the system itself.

Analyses and calculations

The output voltage of the energy generation part and the voltage output of PMS for H_2 evolution were recorded every 30 min by a data acquisition system (2700, Keithley Instruments, OH, USA).[34] The current (I) in both parts were calculated by $I=U/R$ (mA), respectively, where U (mV) was the voltage across a 0.5 Ω resistance and R was 0.5 Ω. Power (P) was calculated from $P=UI$ (mW)[35]. Gases collected in the air bag were tested using a gas chromatograph (Model 8610C, SRI Instruments).[19] Hydrogen volume was calculated by multiplying the total volume of the collected gas with the hydrogen content measured by a gas chromatograph. The chemical oxygen demand (COD), electrolyte conductivity, and pH were measured using the standard methods.[32]

SUPPLEMENTAL INFORMATION

Supplemental Information includes 1 video can be found with this article online.

ACKNOWLEDGMENTS

This work is supported by the US National Science Foundation under award CBET-1834724 and National Renewable Energy Laboratory under Contract No. XFF-8-82229-01. We thank Dianxun Hou for the help on H_2 measurement.

Author Contributions

X.C., F.L.L and Z.J.R. wrote the manuscript. X.C. and F.L.L. conducted the experiment and characterization. Y.B. and L.L. assisted in reactor operation and analyses. X.W.C., M.T., and Y.W. assisted in circuit testing and energy related calculations.

Declaration of Interests

The authors declare no competing interests.

References

1. S. Chu and A. Majumdar, *Nature*, 2012, 488, 294.
2. Z. W. Seh, J. Kibsgaard, C. F. Dickens, I. Chorkendorff, J. K. Nørskov and T. F. Jaramillo, *Science*, 2017, 355, eaad4998.
3. J. A. Turner, *Science*, 2004, 305, 972.
4. A. G. Wallace and M. D. Symes, *Joule*, 2018, 2, 1390-1395.
5. Y. Goto, T. Hisatomi, Q. Wang, T. Higashi, K. Ishikiriyama, T. Maeda, Y. Sakata, S. Okunaka, H. Tokudome, M. Katayama, S. Akiyama, H. Nishiyama, Y. Inoue, T. Takewaki, T. Setoyama, T. Minegishi, T. Takata, T. Yamada and K. Domen, *Joule*, 2018, 2, 509-520.
6. V. Khare, S. Nema and P. Baredar, *Renewable and Sustainable Energy Reviews*, 2016, 58, 23-33.
7. L. Lu and Z. J. Ren, *Bioresour. Technol.*, 2016, 215, 254-264.

8. J. A. Rollin, J. Martin del Campo, S. Myung, F. Sun, C. You, A. Bakovic, R. Castro, S. K. Chandrayan, C.-H. Wu, M. W. W. Adams, R. S. Senger and Y. H. P. Zhang, *Proceedings of the National Academy of Sciences*, 2015, 112, 4964.

9. K. Zeng and D. Zhang, *Prog. Energy Combust. Sci.*, 2010, 36, 307-326.

10. J. Rossmeisl, A. Logadottir and J. K. Nørskov, *Chem. Phys.*, 2005, 319, 178-184.

11. S. Chen, Y. Qi, C. Li, K. Domen and F. Zhang, *Joule*, 2018, 2, 2260-2288.

12. B. Zhang and L. Sun, *Chem. Soc. Rev.*, 2019, 48, 2216-2264.

13. B. E. Logan, D. Call, S. Cheng, H. V. M. Hamelers, T. H. J. A. Sleutels, A. W. Jeremiasse and R. A. Rozendal, *Environ. Sci. Technol.*, 2008, 42, 8630-8640.

14. H. Liu, S. Grot and B. E. Logan, *Environ. Sci. Technol.*, 2005, 39, 4317-4320.

15. A. J. Bard and M. A. Fox, *Acc. Chem. Res.*, 1995, 28, 141-145.

16. N. S. Lewis, *Nature*, 2001, 414, 589.

17. M. G. Walter, E. L. Warren, J. R. McKone, S. W. Boettcher, Q. Mi, E. A. Santori and N. S. Lewis, *Chem. Rev.*, 2010, 110, 6446-6473.

18. L. Lu, N. B. Williams, J. A. Turner, P.-C. Maness, J. Gu and Z. J. Ren, *Environ. Sci. Technol.*, 2017, 51, 13494-13501.

19. L. Lu, W. Vakki, J. A. Aguiar, C. Xiao, K. Hurst, M. Fairchild, X. Chen, F.

448 Yang, J. Gu and Z. J. Ren, *Energy & Environmental Science*, 2019, 12,
449 1088-1099.
450 20. D. Kong, X. Xie, Z. Lu, M. Ye, Z. Lu, J. Zhao, C. S. Criddle and Y. Cui,
451 *Nano Energy*, 2017, 39, 499-505.
452 21. E. Suraniti, P. Merzeau, J. Roche, S. Gounel, A. G. Mark, P. Fischer, N.
453 Mano and A. Kuhn, *Nature communications*, 2018, 9, 3229-3229.
454 22. M. D. Symes and L. Cronin, *Nature Chemistry*, 2013, 5, 403.
455 23. B. Rausch, M. D. Symes, G. Chisholm and L. Cronin, *Science*, 2014, 345,
456 1326.
457 24. V. Amstutz, K. E. Toghill, F. Powlesland, H. Vrubel, C. Comninellis, X. Hu
458 and H. H. Girault, *Energy & Environmental Science*, 2014, 7, 2350-2358.
459 25. A. Landman, H. Dotan, G. E. Shter, M. Wullenkord, A. Houaijia, A.
460 Maljusch, G. S. Grader and A. Rothschild, *Nature Materials*, 2017, 16, 646.
461 26. M. Alaraj, Z. J. Ren and J.-D. Park, *J. Power Sources*, 2014, 247, 636-642.
462 27. F. L. Lobo, X. Wang and Z. J. Ren, *J. Power Sources*, 2017, 356, 356-364.
463 28. H. Wang, J.-D. Park and Z. J. Ren, *Environ. Sci. Technol.*, 2015, 49,
464 3267-3277.
465 29. K. Kazimierczuk Marian, *Kazimierczuk MK. Pulse-width Modulated DC-DC*
466 *Power Converters.*, Wiley, Dayton, Ohio, 2012.
467 30. S. Cheng, H. Liu and B. E. Logan, *Environ. Sci. Technol.*, 2006, 40,
468 364-369.

469 31. D. Hou, A. Iddya, X. Chen, M. Wang, W. Zhang, Y. Ding, D. Jassby and Z.
470 J. Ren, *Environ. Sci. Technol.*, 2018, 52, 8930-8938.
471 32. X. Chen, R. Katahira, Z. Ge, L. Lu, D. Hou, D. J. Peterson, M. P. Tucker, X.
472 Chen and Z. J. Ren, *Green Chemistry*, 2019, 21, 1258-1266.
473 33. X. Chen, H. Sun, P. Liang, X. Zhang and X. Huang, *J. Power Sources*,
474 2016, 324, 79-85.
475 34. Y. Gao, D. Sun, H. Wang, L. Lu, H. Ma, L. Wang, Z. J. Ren, P. Liang, X.
476 Zhang, X. Chen and X. Huang, *Environmental Science: Water Research &*
477 *Technology*, 2018, 4, 1427-1438.
478 35. W. Wang, P.E. Jenkins, Z. Ren, *Corros. Sci.,* 2012, 57, 215-219.
479
480

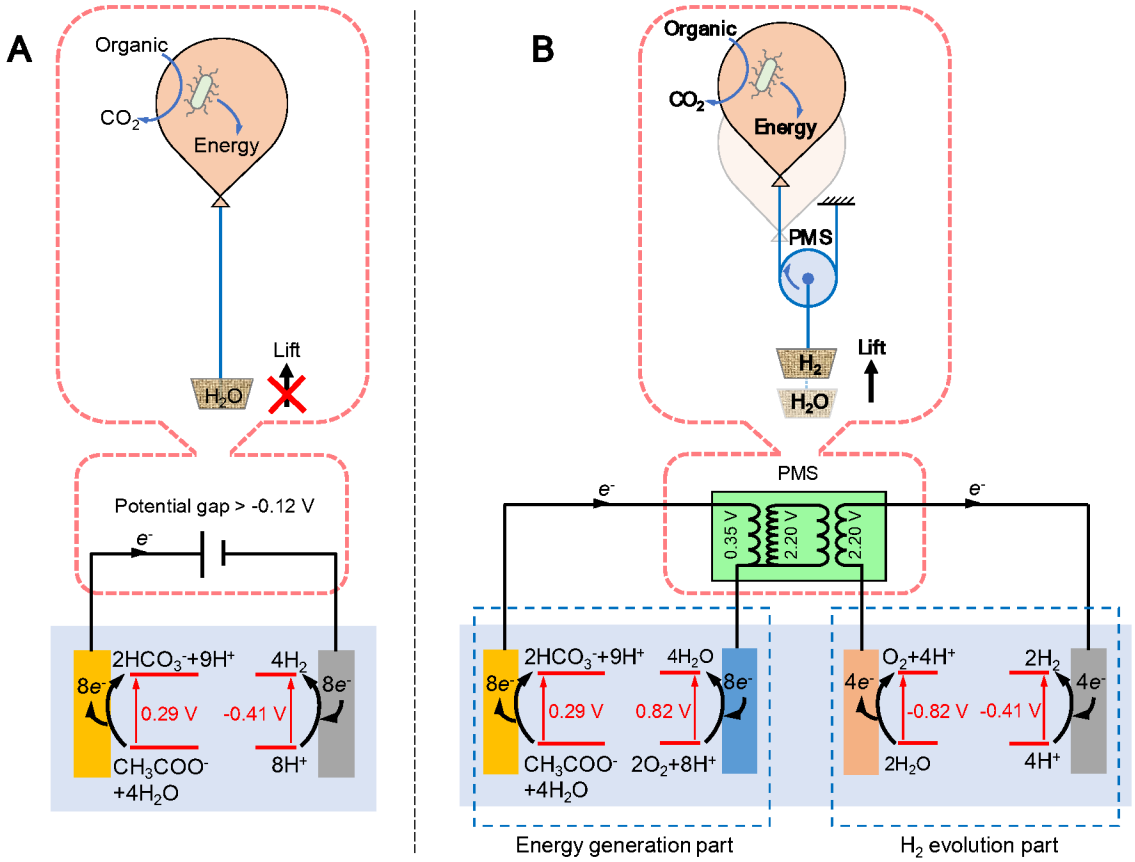

Figure 1 Schematic of the traditional electricity-driven microbial electrolysis H_2 evolution (A) and new spontaneous H_2 evolution enabled by using tailored PMS to decouple the electrochemical reactions (B). Balloon represents the lifting force and basket represents the objective mass to be uplifted. PMS: power management system.

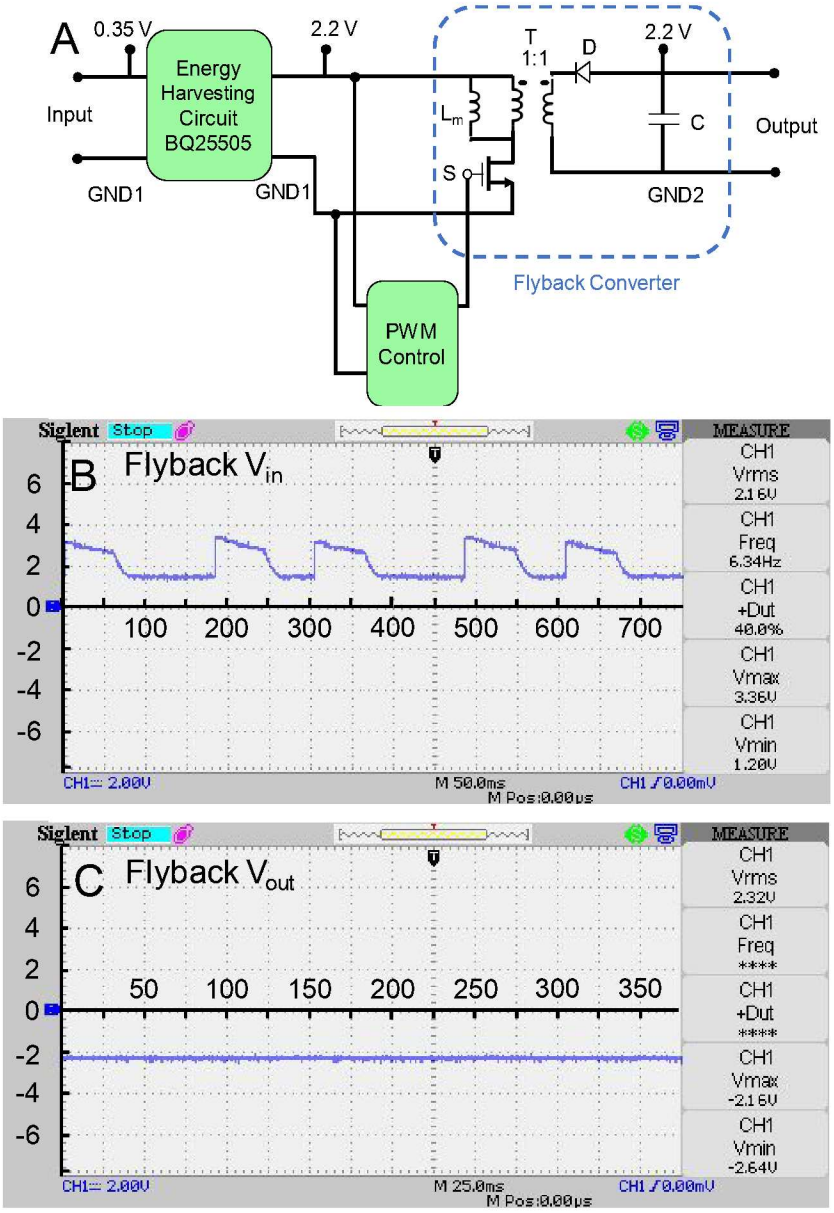

Figure 2 Power management system design (A) and the testing results of the flyback converter input voltage (B) and output voltage (C). The output voltage from the energy harvesting circuit was also the flyback converter input voltage, which was controlled by pulse-frequency modulation using constant duty cycle and variable frequency. PWM: pulse width modulated; (B) and (C) were real-time screen shots of the oscilloscope when testing the input and output voltage of the flyback converter, where Vrms (RMS = root mean square) represented the effective voltage value, +Dut represented the curve positive duty cycle.

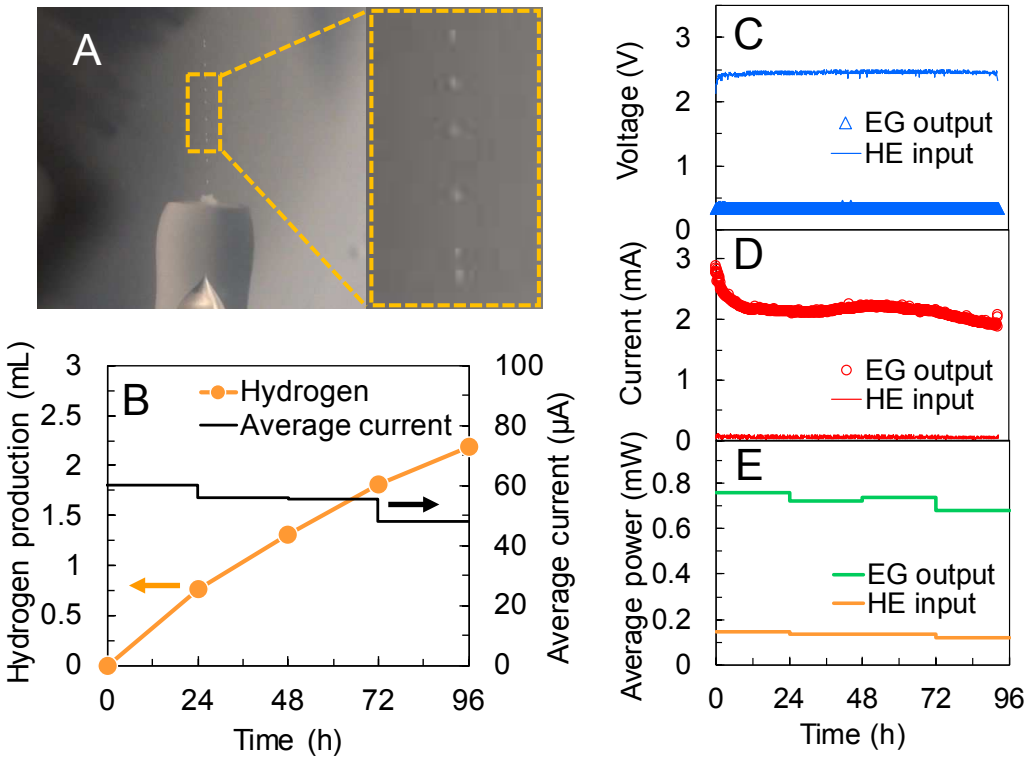

500

501 **Figure 3** Photo showed H_2 bubbles were continuously generated on the cathode
502 without external energy input (A); Hydrogen production and average current in the
503 hydrogen evolution circuit (B); Time-course voltage (C), current (D), and average
504 power (E) of the energy generation part output (EG output) and H_2 evolution part
505 input (HE input).

506

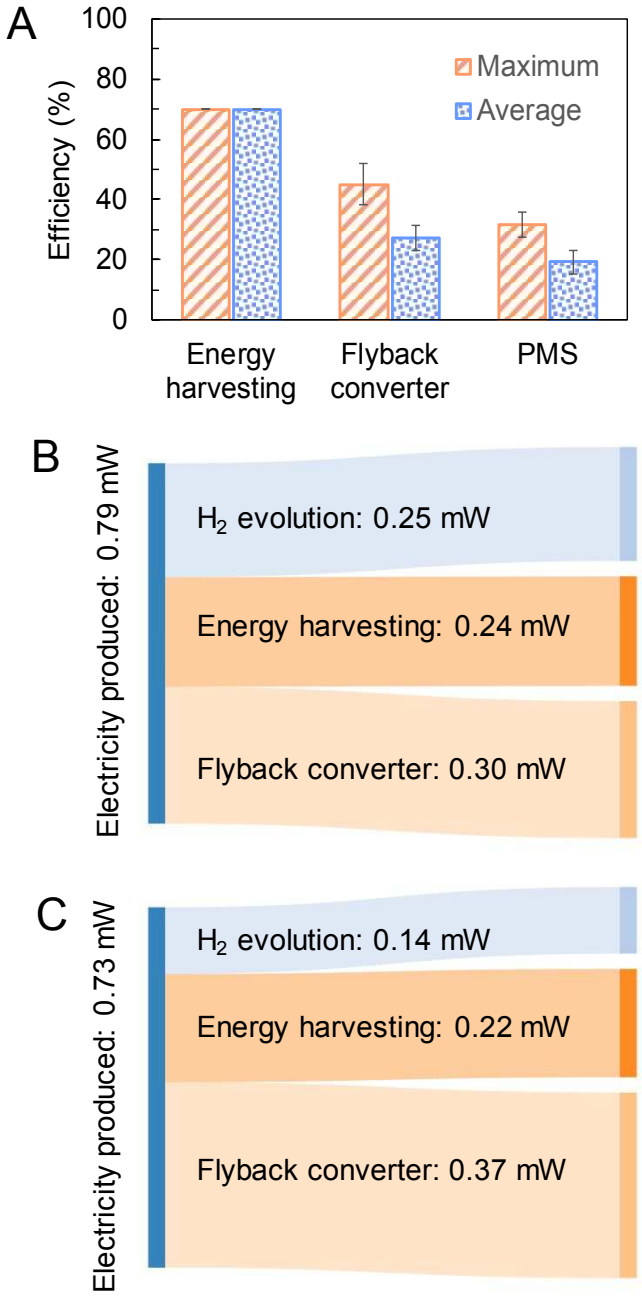

507

508 **Figure 4** Efficiency of the energy harvesting circuit, flyback converter and PMS
509 (A), power flow of the spontaneous H_2 evolution system with maximum PMS
510 efficiency (B) and average PMS efficiency (C).

511